

***In situ* micro-Raman investigation of dehydration mechanism in natural gypsum**

P. S. R. Prasad^{†,*}, A. Pradhan[‡] and T. N. Gowd[†]

[†]Mineral Physics Group, National Geophysical Research Institute, Hyderabad 500 007, India

[‡]Department of Physics, Indian Institute of Technology, Kanpur 208 016, India

The stability of bassanite and the mechanism of dehydration of natural gypsum were investigated by *in situ* micro-Raman spectroscopy in the temperature range 300–380 K and 300–450 K. From the thermal evolution of the sulphate (940–1200 cm⁻¹) and water (3250–3750 cm⁻¹) molecular stretching (ν_1 and ν_3) modes, it was evident that the gypsum dehydrated irreversibly into bassanite at about 370 ± 5 K. We report that this transformation was preceded by the soluble anhydrite phase, with a characteristic Raman shift for $\nu_1(\text{SO}_4)$ to about 1026 cm⁻¹. From the Arrhenius-type variations in the reduced intensities of $\nu_1(\text{SO}_4)$ for bassanite and anhydrite at 1014 cm⁻¹ and 1026 cm⁻¹, respectively, the activation energy for bassanite to anhydrite was estimated to be 32.5 ± 6.6 kJ mol⁻¹.

GYPSUM, a simple hydrous mineral, shows a transition sequence gypsum–bassanite–anhydrite and the phase transitions are construed to be controlled by dehydration and rehydration processes¹. Bassanite ($\text{CaSO}_4 \cdot 0.5\text{H}_2\text{O}$) and γ - CaSO_4 (soluble anhydrite) are the low-temperature (below 383 K) dehydration products of gypsum. γ - CaSO_4 could be rehydrated to form bassanite. However, heating of gypsum above 633 K results in formation of α - CaSO_4 (anhydrite)¹. The water molecules in gypsum are highly interactive with CaO and SO_4 groups and are also essential constituents in the crystallographic arrangement². The volume decrease due to the dehydration of gypsum, increases the porosity and thereby interaction with other fluids of the sediments^{3,4}. Further, this process has impact on its mechanical properties⁵. It was already established that the dehydration phenomenon is more temperature-dependent than pressure-dependent^{1,4,6,7}. In fact, the transition temperature of gypsum to bassanite linearly shifts upwards with pressure⁸. The transition sequence and the individual phases were earlier studied by many techniques, including IR and Raman spectroscopic methods^{1,9–12}. However, there are many unanswered questions, particularly on the stability and the existence of bassanite and other hydrous phases with $2 < \text{H}_2\text{O} < 0.5$. The bassanite is known to be unstable at all the temperatures at one bar pressure¹ and the temperature and pressure above which this phase is stable was estimated to be 85°C and 2 kb,

respectively¹³. On the other hand, most of the experimental results indicate that the dehydration sequence of gypsum follows a stepwise mechanism at ambient pressure. If true, one expects that bassanite would occur commonly as a secondary mineral. However, bassanite is found rarely in nature, and its rare occurrence has been difficult to understand¹⁴. On the other hand, impurities like Sr, Ba, K, Na and Mg are known to play a key role in the formation of gypsum and the dehydration process^{1,15–17}. We undertook a comprehensive study on some natural gypsum samples using *in situ* Raman spectroscopy. Our previous work clearly demonstrated that the sulphate internal modes were sensitive to the phase changes and could effectively be used to probe the structural transitions^{18,19}. Further, the natural alkali and alkaline impurities in gypsum play an active role in the thermal evolution of sulphate modes and onset of dehydration²⁰. Recent studies on synthetic gypsum powdered samples using Raman studies have shown evidences for stepwise dehydration²¹. In this paper, a comprehensive analysis of observed spectral variations in some of the internal modes of sulphate and water molecular groups of natural gypsum are presented with an aim to understand the stability of bassanite and elucidate the mechanism of de(re)hydration, particularly in natural samples.

A small crystal was cut from a large transparent rectangular sheet of gypsum, collected from an unknown salt core location in India and was obtained from M/s Hindustan Minerals and Natural History Specimen Supply Co, Calcutta (India). These samples have been characterized earlier by XRD, Raman and IR spectroscopic methods. Major alkali and alkaline impurities were characterized by XRF. Earlier experimental results on the dehydration of gypsum showed that the dehydration was sequential first to hemihydrate (bassanite) and then to anhydrite. Hemihydrate is known to be thermodynamically unstable at all temperatures; however it is available in nature, although rarely and its existence and formation are difficult to understand. The objective of the present study is to understand the evolution of low temperature dehydration phases (< 383 K), by simultaneously probing Raman modes of sulphate and water molecular groups. The Raman spectroscopic measurements were carried out on the cleaved plane without optical polishing.

The thermogravimetric measurements were conducted in Mettler Toledo Star Systems, using finely-powdered samples, with a heating rate of 2°/min up to 420 K, and thereafter at 20°/min up to 720 K. Similar heating rates have been used by other workers also, who have reported stepwise dehydration²¹. The infrared spectra under ambient temperature and pressure, were recorded on a Nicolet 740 FTIR spectrometer mainly to characterize the starting and dehydrated products of gypsum.

In situ Raman measurements were carried out on a SPEX 1877 Triplemate system, equipped with a liquid nitrogen-cooled CCD detector. Excitation source was

*For correspondence. (e-mail: postmast@csngri.ren.nic.in)

514.5 nm radiation (30 mW) from a SPECTRA PHYSIC 165, 5W argon ion laser. An in-house fabricated variable temperature cell, which could go up to 520 K, with an accuracy better than ± 5 K, was used for phase transition studies. A copper–constantan thermocouple was mounted in close proximity of crystal to monitor its temperature. The relative humidity of the surroundings was about 60%. The typical rates at which the temperature of the sample was increased/decreased were lower than $1^\circ/\text{min}$. The sample was irradiated along y -axis with the laser radiation and back-scattered radiation was collected. The uncertainty in the intensity and peak position for sharp and strong Raman bands is about 10% and $\pm 1\text{ cm}^{-1}$, respectively, and the same for weak and broad bands could be up to 15% and $\pm 5\text{ cm}^{-1}$.

A natural gypsum sample, used in the present study, was earlier characterized by XRF, infrared (IR) and Raman spectroscopic techniques^{18,20}. The observed vibrational modes were compared with the previously published values^{9,12}. The unit cell parameters from XRD studies were found to be $a = 5.68\text{ \AA}$, $b = 15.18\text{ \AA}$, $c = 6.51\text{ \AA}$ and $\beta = 118.4^\circ$ with $Z = 4$. The space group is $I2/a$ (C_{2h}^6) which is in agreement with that of Pedersen and Semmingsen²².

From the thermogravimetric study it was found that the dehydration of gypsum which started slowly at about 356 K became rapid at higher temperatures (Figure 1). This process was almost completed at around 396 K. From Figure 1, total mass loss during the dehydration process is about 20%. This mass change is higher than that expected for gypsum to bassanite transition. Interestingly we have not observed any other mass change till about 720 K.

In situ Raman studies were carried out with two main aims. Firstly, to understand the stability of bassanite phase

formed due to the dehydration of gypsum. Secondly, to understand the mechanism of dehydration and rehydration sequence in natural gypsum. So the experiment was conducted in two steps. In step 1, the sample was heated only up to a temperature (380 K) where it started to dehydrate and was cooled back to ambient temperature. In step 2, partially dehydrated gypsum from step 1 (kept under ambient conditions for about 72 h, although at a heating rate of $1^\circ\text{C}/\text{min}$ and soaking time of 15 min is adequate to complete the process under ambient conditions) was re-heated to 450 K, till it dehydrated. Some thermosensitive Raman modes of the sulphate and water molecules were monitored at various temperatures during heating and cooling cycles to understand the process.

Observed thermal evolution of ν_1 and ν_3 modes of sulphate and water molecular groups during gypsum to bassanite transition is shown in Figure 2 *a* and *b*, respectively. The spectral traces 1–4 (from the bottom) were recorded during increasing temperature, while traces 5 and 6 were during the cooling cycle. These traces were recorded at temperatures 300, 335, 358, 371, 358 and 300 K, respectively. Temperature of the sample was varied at a rate less than $1^\circ/\text{min}$ and soaking time was about 15 min. Spectral profiles at different temperatures were deconvoluted into minimum number of Lorentzian lines with the help of lab-calc software (Galactic Industries Corp., USA) and the best-fitted parameters were used for further analysis¹⁹. It is clear from Figure 2 *a* that the characteristic $\nu_1(\text{SO}_4)$ mode of gypsum, appeared around 1008 cm^{-1} in this sample and shifted abruptly to higher wavenumber (1026 cm^{-1}) at around 370 K, with an appreciable decrease in the peak intensity. The $\nu_3(\text{SO}_4)$ mode which appeared at around 1141 cm^{-1} in gypsum shifted upwards and split into two peaks at 1148 and 1171 cm^{-1} , around 370 K. This structure largely remained

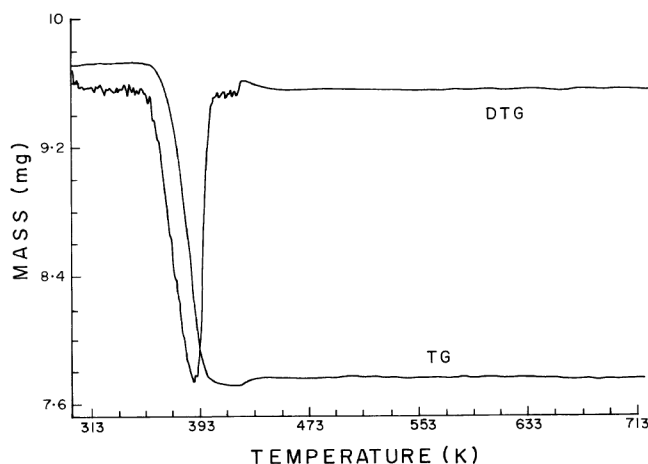


Figure 1. Thermogravimetric (TG) and differential thermogravimetric (DTG) traces of gypsum up to 720 K. The heating rates are $2^\circ/\text{min}$ and $20^\circ/\text{min}$, respectively, in the temperature range 300–420 and 420–720 K.

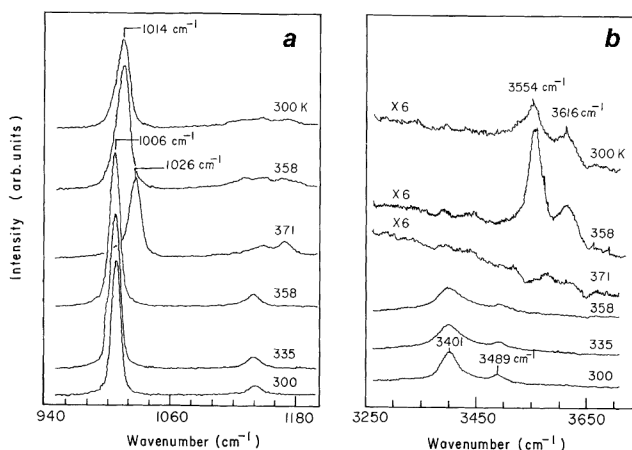


Figure 2. Raman spectra of gypsum in (a) sulphate and (b) water stretching mode regions at various temperatures. Traces 1–4 (from the bottom) are during heating and 5 and 6 are during cooling cycles. Traces 1–3 show the characteristic features of gypsum, whereas the features in trace 3 and traces 4 and 5 correspond to soluble anhydrite and bassanite, respectively.

as such when the temperature was decreased to 300 K. The $\nu_1(\text{SO}_4)$ mode on the other hand stabilized at around 1014 cm^{-1} on cooling. The sample completely lost its transparency and turned opaque and these spectral features were retained even after keeping the sample at ambient temperature for a longer time (approx. 72 h).

The observed spectral changes in the water stretching mode region were even more prominent (Figure 2 *b*). The two Raman modes observed around 3401 and 3489 cm^{-1} in gypsum (in trace 1) were earlier assigned to ν_1 and ν_3 modes of water molecules¹². Interestingly the spectral variations associated with both the sulphate and water molecular groups were observed at the same temperature. On cooling, corresponding modes appeared around 3554 and 3616 cm^{-1} , respectively (trace 6, Figure 2 *b*). The background level also increased sharply around 370 K. The spectral traces 4–6 were recorded at 6 times higher acquisition times.

In step 2, the dehydrated gypsum was re-heated to 450 K. The spectral variations in the ν_1 and ν_3 modes of sulphate and water observed at temperatures 300, 373, 425, 445, 372 and 303 K (from the bottom) are shown in Figure 3. It is interesting to note that the $\nu_1(\text{SO}_4)$ mode which shifted to 1026 cm^{-1} at around 373 K, has not shown any further wavenumber shift at higher temperatures. The $\nu_3(\text{SO}_4)$ doublet at room temperature in this case, has not shown much variation, except that an additional broad mode appeared at 1115 cm^{-1} around 425 K. With increasing temperature these modes became weaker and broader. The weaker $\nu_1(\text{H}_2\text{O})$ and $\nu_3(\text{H}_2\text{O})$ modes at about 3552 and 3611 cm^{-1} , respectively, as shown in Figure 3 *b*, disappeared at elevated temperatures and reappeared on cooling without shift.

Gypsum dehydrates to bassanite by losing one and half of its crystalline water at high temperature¹. The exuded water molecules leave behind some voids in the crystal

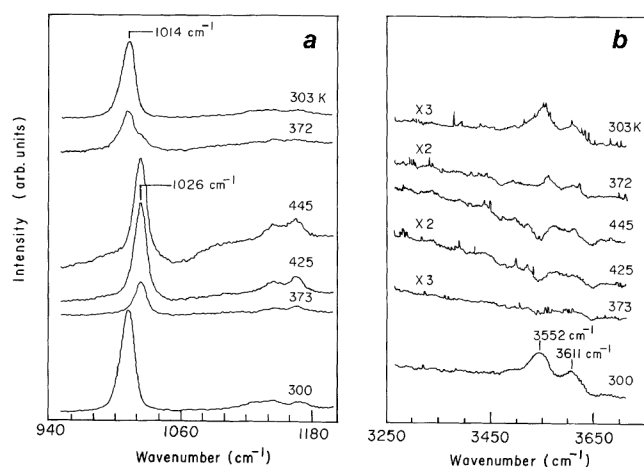


Figure 3. Thermal evolution of ν_1 and ν_3 modes of (a) sulphate and (b) water groups of bassanite (dehydrated gypsum). Traces 1–4 (from the bottom) are during heating and traces 5 and 6 are during cooling cycles. Characteristic Raman bands for bassanite are observed in traces 1, 5 and 6. Spectral traces for soluble anhydrite are in 2–4.

structure. The voids could be filled in by the other constituents like sulphate and calcium groups and/or some impurities that may co-exist with gypsum. On the stability of various gypsum phases, it was suggested that the gypsum should dehydrate into anhydrite at one bar pressure and that bassanite should be unstable at all temperatures at ambient pressure^{1,13}. Further, a detailed analysis of pressure dependence of the onset temperature (T_c) for gypsum to bassanite transition indicated a linear upward shift for T_c with pressure⁸. Extrapolating this behaviour to ambient pressures resulted in higher T_c than that observed experimentally (370 K), which the authors⁸ attributed to some additional mechanism. However, all the experiments reported so far indicate a stepwise dehydration reaction from gypsum to bassanite. From Figure 3 *a* it is clear that the $\nu_1(\text{SO}_4)$ mode, which appeared around 1008 cm^{-1} , had shown interesting variations with temperature. The peak position and reduced intensity variations in $\nu_1(\text{SO}_4)$ mode were systematically plotted in Figure 4. From Figure 4 *a*, it appears that the peak position shifted abruptly to 1026 cm^{-1} with a small asymmetric peak around 1016 cm^{-1} , at about 370 K. On decreasing the temperature, the peak around 1026 cm^{-1} disappeared and the asymmetry around 1016 cm^{-1} developed into a stronger band. Further, the $\nu_1(\text{H}_2\text{O})$ and $\nu_3(\text{H}_2\text{O})$ observed at around 3401 and 3489 cm^{-1} in gypsum phase (Figure 3 *b*), completely disappeared at around 370 K and reappeared at around 3552 and 3611 cm^{-1} on cooling. Earlier Raman spectroscopic studies at ambient conditions on calcium sulphate

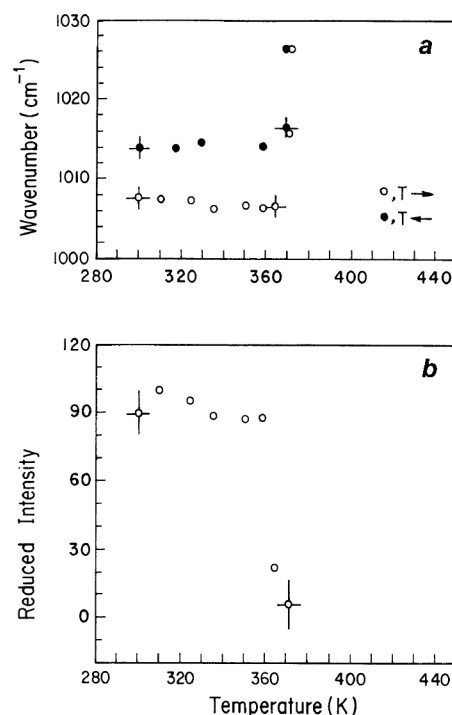


Figure 4. (a) Peak positions and (b) reduced intensity variations with temperature in $\nu_1(\text{SO}_4)$ mode of gypsum. Experimental uncertainties are shown only on a few points for clarity.

hydrates indicated that the $\nu_1(\text{SO}_4)$ mode in bassanite occurs at around 1018 cm^{-1} , while the corresponding mode for the soluble anhydrite appears at 1020 cm^{-1} (refs 23 and 24). Our observations of $\nu_1(\text{SO}_4)$ at a shifted position (compared to gypsum at 1008 cm^{-1}) at 1014 cm^{-1} and $\nu_1(\text{H}_2\text{O})$ and $\nu_3(\text{H}_2\text{O})$, respectively, at around 3552 and 3611 cm^{-1} indicate that the dehydrated (heated up to 370 K and cooled) product could be the bassanite. A split in the Raman bands at 1152 and 1174 cm^{-1} for $\nu_3(\text{SO}_4)$ corroborates this fact. Further, $\nu_1(\text{H}_2\text{O})$ and $\nu_3(\text{H}_2\text{O})$ modes shifted upwards with increasing temperature, indicating an increase in $(\text{OH} \cdots \text{O})$ bond distance (i.e. weaker hydrogen bonding) in bassanite. We observed the same spectral features as described, even after 72 h of cooling, indicating that the bassanite was not rehydrated rapidly to form gypsum under these experimental conditions.

Another interesting feature in the heating cycle was the appearance of 1026 cm^{-1} ($\nu_1(\text{SO}_4)$) band along with the disappearance of (OH) modes prior to the onset of spectral features typical of bassanite. From Table 1 it is clear that all other weaker modes of sulphate tetrahedra are comparable to the corresponding modes observed at ambient conditions by Bensted²³. Apparently not many spectroscopic studies are reported in the literature with a distinctive feature for soluble and insoluble anhydrites. Small variations in the Raman band positions for sulphate tetrahedra observed in the present study could tentatively be attributed to the higher temperature. All these Raman spectral anomalies observed at around 370 K could be attributed to the following: during dehydration, gypsum loses all its crystalline water and then the water molecules required for the formation of bassanite re-enter into the structure.

There are many unanswered questions regarding the formation and stability of bassanite. It is known to be unstable at ambient conditions and even if it does form, it should dehydrate to anhydrite at higher temperatures. We are unaware of any attempts to verify the reversibility of this dehydration sequence under similar experimental conditions. From the thermal evolution of the Raman

bands shown in Figure 3, it is clear that the spectral features typical of anhydrite started appearing around 360 K , and around 445 K spectral features typical of bassanite phase were completely replaced by those of anhydrite. However, on cooling the spectral features of bassanite were recovered, indicating that the bassanite to anhydrite transition is reversible under our experimental conditions. Further, FTIR spectra on the end product of the reaction has shown all the characteristic features of bassanite, namely $\nu_1(\text{H}_2\text{O})$, $\nu_2(\text{H}_2\text{O})$ and $\nu_3(\text{H}_2\text{O})$ bands, respectively at 3560 , 1621 and 3615 cm^{-1} .

The spectral parameters of $\nu_1(\text{SO}_4)$ mode of bassanite showed interesting variations with temperature, as plotted in Figure 5. A new mode appeared at 1026 cm^{-1} around 360 K and became stronger at higher temperatures. At about 425 K , the characteristic mode of bassanite (1014 cm^{-1}) disappeared, while that of anhydrite at 1026 cm^{-1} persisted (Figure 5 a). The reduced intensity of the band (defined as $I_{\text{tp}} = I_{\text{op}} w_p / \{n(w) + 1\}$ where I_{op} is the observed peak intensity at w_p and $n(w)$ the Bose–Einstein population factor) around 1014 cm^{-1} decreased, while that around 1024 cm^{-1} increased with temperature (Figure 5 b). This variation was fitted to an Arrhenius-type relation to estimate the activation energy associated with the transition (Sarma *et al.*¹⁸). From the intensity variations in both the bands, we estimated the activation energy to be 31.87 ± 8.1 and $32.46 \pm 6.6\text{ kJ mol}^{-1}$, respectively (Figure 5 c). These values are in close agreement with those in previously published reports^{18,25}, i.e. 32.94 and 28.00 kJ mol^{-1} , respectively.

On decreasing the temperature the spectral features in the Raman spectra of bassanite were recovered. The $\nu_1(\text{SO}_4)$ mode appeared at 1014 cm^{-1} and $\nu_3(\text{SO}_4)$ mode, which split into three components in the anhydrite, merged into two bands at 1152 and 1174 cm^{-1} . More interestingly, the $\nu_1(\text{H}_2\text{O})$ and $\nu_3(\text{H}_2\text{O})$ re-appeared at around 3554 and 3616 cm^{-1} (Figure 3 b). These results clearly demonstrate that bassanite dehydrates into anhydrite in a reversible fashion.

Table 1. Observed Raman band positions (cm^{-1}) of sulphate group in dehydrated products of natural gypsum, i.e. $\text{CaSO}_4 \cdot n\text{H}_2\text{O}$

<i>n</i>	ν_1	ν_2	ν_3	ν_4
<i>Gypsum</i>				
2.0 ^a	1008	420, 494	1141	623
2.0 ^b	1010	414, 494	1114, 1138, 1144	622, 624, 676
<i>Bassanite</i>				
0.5 ^a	1014	421, 490	1152, 1174	630, 680
0.5 ^b	1018	438, 494	1132, 1150, 1174	602, 636, 676
<i>Anhydrite</i>				
0.0 ^{a,@}	1026	424, 490	1105 (vb), 1152, 1174	608, 628, 668, 685
0.0 ^b	1020	438, 498	1131, 1150, 1172	611, 630, 679

^aPresent study; [@]Observed at temperature 425 K ; vb, Very broad; ^bFrom Bensted²³.

OH stretching modes in gypsum are at 3401 and 3489 cm^{-1} and those of bassanite at 3554 and 3616 cm^{-1} .

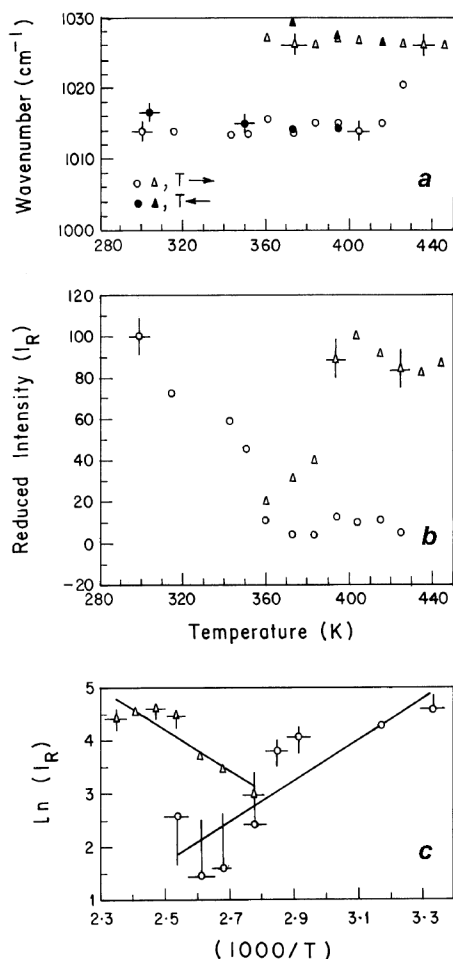


Figure 5. Temperature-induced variations in (a) peak position and (b) reduced intensity (I_R) of the characteristic $\nu_1(\text{SO}_4)$ modes of bassanite (1014 cm^{-1} , \circ) and anhydrite (1026 cm^{-1} , Δ). Open (\circ , Δ) and closed (\bullet , \blacktriangle) symbols are for the temperature increasing and decreasing cycles, respectively. $\ln(I_R)$ as a function of inverse temperature is plotted in (c) to estimate the activation energy.

In summary, our *in situ* micro-Raman studies on natural gypsum provided the following information about the dehydration-induced transition sequence:

(a) Gypsum dehydrates into bassanite at around 370 K and it was an irreversible change at ambient pressure; (b) The formation of bassanite by the dehydration of gypsum occurs through an intermittent soluble anhydrite phase, which was not discovered earlier. In other words, the entire water of crystallization of gypsum becomes detached from the structure and then the required water molecules ($0.5\text{H}_2\text{O}$) re-enter into the crystal structure to form bassanite. However, careful *in situ* XRD studies could provide more insight into the phenomenon; (c) It appears that bassanite formed from the dehydration of gypsum is stable and does not rehydrate to form gypsum

under our experimental conditions. Even if it rehydrates to gypsum, it might occur on longer time scales; (d) Bassanite dehydrates into soluble anhydrite with characteristic Raman mode for $\nu_1(\text{SO}_4)$ around 1026 cm^{-1} and this reaction is reversible as long as the temperature does not exceed 633 K (a point where it transforms into insoluble anhydrite).

1. Zussman, J., in *Rock Forming Minerals: Sulphates, Carbonates, Phosphates and Halides* (eds Chang, L. L. Y., Howie, R. A. and Zussman, J.), Longman, Harlow, 1996, vol. 5B.
2. Lager, G. A., Armbruster, F. J. Th., Rotella, J. D. and Hinks, Jorgensen, D. G., *Am. Miner.*, 1984, **69**, 910–918.
3. Warren, J. K., *Evaporite Sedimentology: Importance to Hydrocarbon Deposition*, Prentice Hall, New Jersey, 1989.
4. Stretton, I. C., Schofield, P. F., Hull, S. and Knight, K. S., *Geophys. Res. Lett.*, 1997, **24**, 1267–1270.
5. Murrell, S. A. F. and Ismail, I. A. H., *Tectonophysics*, 1976, **31**, 207–258.
6. Schofield, P. F., Knight, K. S. and Stretton, I. C., *Am. Mineral.*, 1996, **81**, 847–851.
7. Couty, R., Velde, B. and Besson, J. M., *Phys. Chem. Mineral.*, 1983, **10**, 89–93.
8. McConnell, J. D. C., Astill, D. M. and Hall, P. L., *Mineral. Mag.*, 1987, **51**, 453–457.
9. Bensted, J. and Prakash, S., *Nature*, 1968, **219**, 60–61.
10. Putnis, A., Winkler, B. and Fernandez-Diaz, L., *Mineral. Mag.*, 1990, **54**, 123–128.
11. Berenblut, B. J., Dawson, P. and Wilkinson, G. R., *Spectrochim. Acta A*, 1973, **29**, 29–36.
12. Krishnamurthy, N. and Soots, V., *Can. J. Phys.*, 1971, **49**, 885–896.
13. Yamamoto, H. and Kennedy, G. C., *Am. J. Sci. A*, 1969, **267**, 550–557.
14. Akpokodje, E. G., *Chem. Geol.*, 1984/1985, **47**, 361–364.
15. Toulkeridis, T., Podwojewski, P. and Clauer, N., *Chem. Geol.*, 1998, **154**, 61–71.
16. Kushnir, J., *Geochim. Cosmochim. Acta*, 1980, **44**, 1471–1482.
17. Ostroff, A. G., *Geochim. Cosmochim. Acta*, 1964, **28**, 1363–1372.
18. Sarma, L. P., Prasad, P. S. R. and Ravikumar, N., *J. Raman Spectrosc.*, 1998, **29**, 851–856.
19. Prasad, P. S. R., *J. Raman Spectrosc.*, 1999, **30**, 693–696.
20. Prasad, P. S. R., Ravikumar, N., Krishnamurthy, A. S. R. and Sarma, L. P., *Curr. Sci.*, 1998, **75**, 1410–1414.
21. Chang, H., Huang, P. J. and Hou, S. C., *Mater. Chem. Phys.*, 1999, **58**, 12–19.
22. Pedersen, B. F. and Semmingsen, D., *Acta Crystallogr. B*, 1982, **38**, 1074.
23. Bensted, J., *J. Am. Ceram. Soc.*, 1976, **59**, 140.
24. Kosztolanyi, C., Mullis, J. and Weidmann, M., *Chem. Geol.*, 1987, **61**, 19–28.
25. Winkler, B., *Phys. Chem. Miner.*, 1996, **23**, 310–318.

ACKNOWLEDGEMENTS. We thank Dr H. K. Gupta, Director, National Geophysical Research Institute, for his encouragement and keen interest in this work and for permission to publish this paper. We also thank Dr R. N. Panda for help during the experiments and Dr L. P. Sarma for useful discussions.

Received 7 December 2000; revised accepted 23 January 2001